

# The effect of carbon nanotube concentration on the physical properties of CNT-polycarbonate composites

M. M. LARIJANI<sup>a,\*</sup>, E. J. KHAMSE<sup>a,b</sup>, J. DAVOODI<sup>b</sup>, F. ZIAIE<sup>a</sup>, S. SAFA<sup>a</sup>, K. ARBABI<sup>a</sup>, M. A. TAGHAVIZADEH<sup>c</sup>

<sup>a</sup>Agricultural Medical and Industrial Research School, Nuclear Science and Technology

Research Institute (NSTRI), Karaj, Iran

<sup>b</sup>Department of Science, Zanjan University, Zanjan, Iran

<sup>c</sup>Radiation Processing School, NSTRI, Iran

Effects of incorporation of multi-walled carbon nanotubes (MWCNTs) as filler into polycarbonate (PC) on the optical, mechanical and electrical properties of MWCNT/PC nanocomposites are presented. The electrical results were achieved using four point probe technique suggesting that two percolation thresholds could coexist in a nanocomposite based on thermoplastic matrix as the insulator like thermoset ones. The conductivity change is more significant in the higher one than the lower one. Detailed calculations at concentrations above the second threshold show a better scaling law dependence of the conductivity on the filler load (with an exponent of 3.7) than its below level (with an exponent of 1.09).

(Received December 7, 2010; accepted March 16, 2011)

**Keywords:** Carbon nanotubes, Polymer–matrix composites (PMCs), Electrical properties

## 1. Introduction

Flexible transparent polymer-based composites have widely overcome the use of glass as they show exclusive properties such as resistance to cracking, low weight and also easy design and process [1]. Most of the earlier studies are related to the different properties of polymer/carbon nanotube composites especially in terms of mechanical and electrical properties [2]. Reinforcement with CNTs is attributed to excellent stiffness and conductivity of CNTs that lead to new materials with fewer hazards of fracture and electrostatic charging in automobile, aerospace and electronic industries [3]. CNTs are remarkably stiffer and stronger than other carbon allotropic types because of their smaller diameter and their less probability of failure when the cracks are generated during fabricating and loading [1].

Since the inter-tube Van der Waals interactions make distinct CNTs to aggregate together, the uniform dispersion of carbon nanotubes in matrix plays an important role in achieving maximum conductivity, transparency and satisfactory mechanical properties. Bauhofer et al [4] by reviewing experimental results demonstrated that the conductivity caused by non-entangled multi-walled CNTs (MWCNTs) is 50 times more than the entangled ones.

Considering the importance of CNTs' homogenous dispersion in matrix, several strategies have been implemented to improve both compatibility and dispersion of CNTs into polymer matrix such as: ultrasonication, molding, and hot pressing.

Among many fabrication methods of polymer/CNT composites, solution casting provides best dispersion of CNTs at the same loading, but its limitation is related to the use of higher loading [1]. In spite of lots of recently

published papers [5-7] on characterization of PC/CNT composites, an overall research is needed to make it possible for apply them in industrial scale (like windowing) as antistatic transparent materials with good mechanical properties.

In this paper we have presented our data for mechanical properties and transparency of PC/CNT composites synthesized employing easy solution casting method under various CNT concentrations. The resistivity of these composites was also studied via standard four point probe technique.

## 2. Experimental

Based on the target thickness and filler concentration of composites, the films of 20  $\mu\text{m}$  thickness were prepared as follows:

Certain amounts of PC were individually dissolved in chloroform using magnetic heater stirrer. Considering the amount of dissolved PCs, certain weight percentage of MWCNTs was dispersed in chloroform separately via ultrasonication for 60 min (summarized in Table 1). In order to get more homogeneous solvents, the resulted solutions were then mixed together and sonicated. Subsequently, the solutions were cast in different dishes (diameter of 6 cm) and to prevent crystallization, chloroform was distilled rapidly over hotplate at 50 °C. Completely dried samples were put into conventional oven at 80°C to remove remained solvent perfectly.

It should also be mentioned that before dispersion, some analyses such as thermogravimetric analysis (TGA) with a Rheometric Scientific SDA 1500 apparatus and Raman spectroscopy analysis with the Jobin LabRam HR-800 Stokes mode with 532 nm frequency-doubled

Nd:YAG laser excitation were carried out to evaluate the quality of the MWCNTs.

To observe dispersion and MWCNT agglomeration in PC matrix, the micrographs of the cryogenically cut films

were obtained from scanning electron microscopy (SEM, model LEO 440i).

Table 1. Theoretical and experimental values of various CNT/PC composite moduli as a function of CNT.wt%.

Sample	CNTs (Wt%)	CNTs (V %)	$E_1^a$ (GPa)	$E_2^b$ (GPa)	$E^c$ (GPa)	$E_{exp}$ (GPa)
Neat PC	0	0	-----	-----	-----	1.32
A	0.05	0.033	1.098	1.001	1.369	1.41
B	0.1	0.067	1.196	1.002	1.419	1.44
C	0.3	0.200	1.590	1.006	1.617	1.50
D	0.5	0.334	1.984	1.010	1.815	1.49

<sup>a</sup> extracted from relation (1)

<sup>b</sup> extracted from relation (2)

<sup>c</sup> extracted from relation (3)

UV-visible spectrophotometer (BECKMAN DU 640) was also used to investigate the transparency of the films (without eliminating the PC raw effects) in the range of 400-800 nm wavelengths.

As shown in (Fig. 1), to measure the electrical properties of PC/MWCNT composites four point probe measurement was applied. Thus, the sample surface was coated with rod shape copper layer ( $2 \times 14 \text{ mm}^2$ ) using magnetron sputtering method. The electrometer (GTM unit) was used to measure the current. To study the mechanical properties of the composites, the standard tensile test was carried out with strip shape specimen on a Hiwa 200 system at a crosshead speed of 50 mm/min using ASTM D882-02 protocol under room temperature conditions and each value reported was the average of at least three samples.

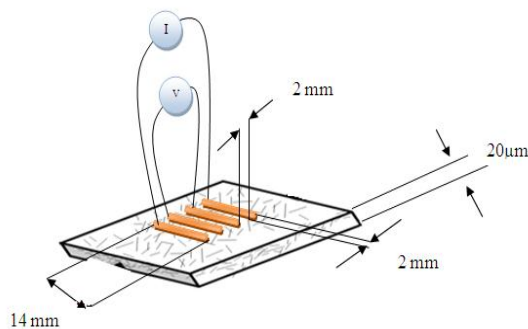


Fig. 1. Schematic view of four point probe analysis.

The specimens were 10 mm in width, gauge length was set to 30 mm and thickness of the specimens ranged from 15~20  $\mu\text{m}$ . The specimens were prepared with laser cutting machine. The Young's modulus of the specimens was extracted from the stress – strain graph. Optical

images of samples were obtained from Dino/Lite digital microscope.

### 3. Results and discussion

#### 3.1. MWCNT characterization

The MWCNTs were purchased from Plasma Chem. GmbH, Inc<sup>TM</sup>. (www. plasmachem.com) with 10-20 nm diameter, 1-10  $\mu\text{m}$  length and > 98% purity. Aspect ratio, ratio of length to diameter of CNTs (L/d), is approximately 1000. (Figs. 2 and 3) show the TGA and Raman spectroscopy results of MWCNTs, respectively.

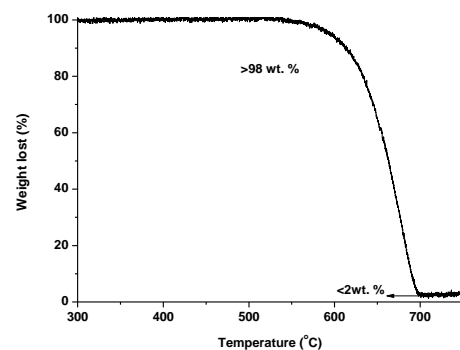


Fig. 2. TGA graph of carbon nanotubes.

From thermogravimetric analysis (Fig. 2), the amorphous carbon and catalyst nano particle as impurities were estimated to be less than 2 wt. % which represents the CNTs high level of purity. According to the Raman spectroscopy (Fig. 3), the lack of a broad peak between D and G bands indicates a very low amount of amorphous carbon in sample [8].

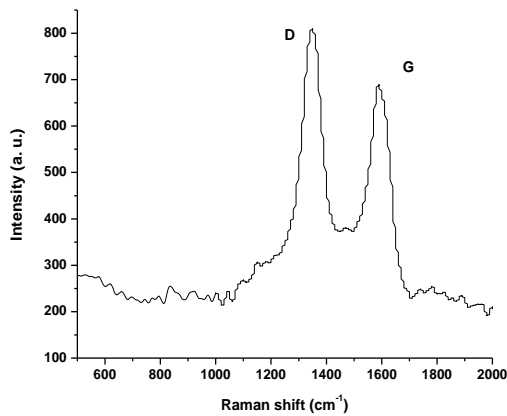


Fig. 3. Raman spectra of carbon nanotubes.

### 3.2 Optical measurement

Fig. 4 illustrates the optical transmission spectra (T) of the samples which differ in their MWCNT concentration. As it can be seen, the transmittance of the neat PC slowly decreases with increasing MWCNT concentration in the polymer-based composite.

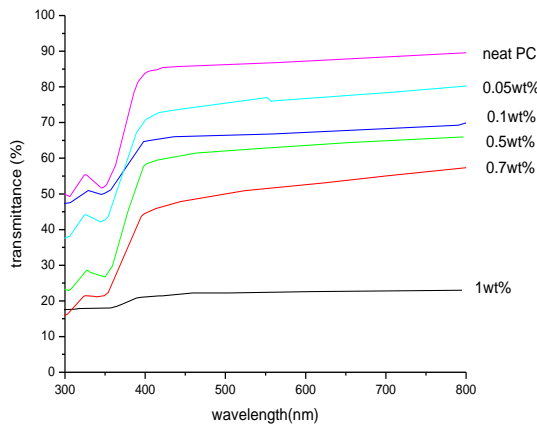


Fig. 4. Optical transmittance of MWCNT/PC composite contains various amounts of MWCNTs.

While passing light through material, it will be scattered from its origin passage if the particle size is larger than the wavelength of visible light and the object seems opaque, otherwise the particle will not affect the passage of light and the material can appear transparent. Since CNTs tend to aggregate, increasing their amount in matrix increases the bundle radius and as a result, the materials transparency decreases. The images in (Fig. 5) show the samples with 0.1 (Fig. 5a) and 1wt% (Fig. 5b) of CNT that emphasize the above mentioned issue

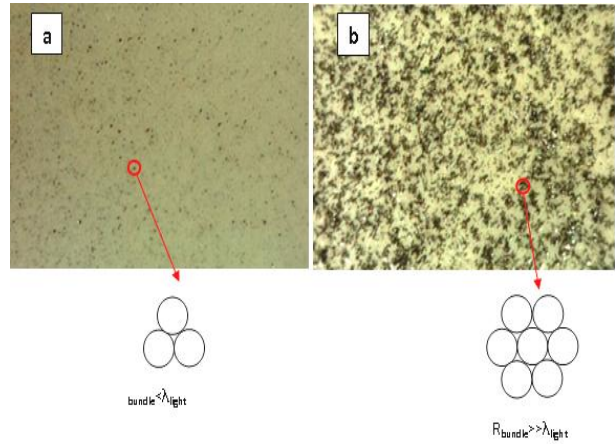


Fig. 5. Optical microscopy images of (a) 0.1wt% and (b) 1wt% of CNT. R is the diameter of created bundles.

It is worthwhile to note that the transmittance more than 70% is acceptable for glass related applications and the maximum CNT concentration for a transparent film is estimated to be 0.1 wt % MWCNTs approximately.

### 3.3 Mechanical properties

#### 3.3.1 Calculation of MWCNT/PC mechanical properties

Among various models for estimate the mechanical properties of randomly oriented discontinuous short fiber composites; Halpin-Tsai [9] is the most adequate equation for experimental results. They developed the following approximate expression for isotropic lamina to find the mechanical constant composites:

$$E = 3/8E_1 + 5/8E_2 \tag{1}$$

where E, E<sub>1</sub> and E<sub>2</sub> are denoted to total, longitudinal and transverse modulus of elasticity, respectively. Assuming the equal applied stress for composite, matrix and fiber, longitudinal modulus of elasticity is calculated using:

$$\frac{E_1}{E_m} = \frac{1 + 2\frac{L}{d}\eta v_f}{1 - \eta v_f}, \quad \eta = \frac{\left(\frac{E_f}{E_m} - 1\right)}{\left(\frac{E_f}{E_m} + 2\frac{L}{d}\right)} \tag{2}$$

and modified Halpin-Tsai is applied to find the transverse one:

$$\frac{E_2}{E_m} = \frac{1 + 2\eta v_f}{1 - \eta v_f}, \quad \eta = \frac{\left(\frac{E_f}{E_m} - 1\right)}{\left(\frac{E_f}{E_m} + 2\right)} \tag{3}$$

where E<sub>m</sub> and E<sub>f</sub> are Young's moduli of matrix and filler respectively and v<sub>f</sub> is volume fraction of CNTs in matrix. The amount of E<sub>m</sub> has been calculated by standard tensile test and E<sub>f</sub> value has been extracted from the literatures [10-12]. To convert weight fraction to volume fraction for CNT, the reported equations in ref [13] were used in which the density of polycarbonate matrix and CNT have been considered to be 1.2 and 1.8 gr/cm<sup>3</sup>, respectively. In

the above relations, the mismatch between longitudinal and transverse modulus of elasticity for CNTs is ignored and the strength of MWCNT due to covalent C-C bond is approximately equal for two perpendicular stresses. This could result in highly strength isotropic composite unlike the graphite fiber composites which are extremely strong in longitudinal and so weak in transverse [14]. (Table 1) represents the other derived and experimental properties of the composites.

### 3.3.2 Tensile experience

Fig. 6 represents the experimental Young's modulus of the neat PC and MWCNT reinforced composites in comparison with the theoretical model.

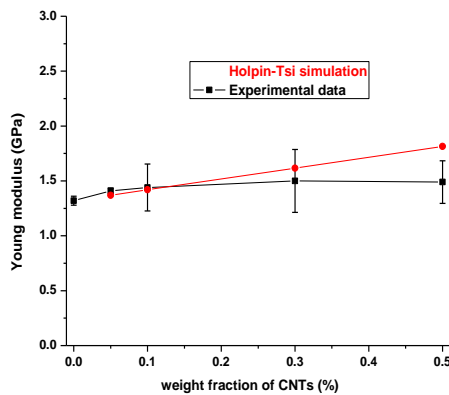


Fig. 6. Experimental-theoretical Young's modulus of PC/MWCNT composites.

The measured modulus of composites is nearly the same as theoretical ones up to 0.13 wt%. Afterwards, the difference between theoretical and experimental values is increased. This indicates that MWCNT dispersion gets worse when the MWCNT loading exceeds 0.13 weight per cent. It is due to MWCNT aggregation that inhibits the improvement of composite mechanical properties. Singh et al [15] reported that the maximum achievable elastic modulus is approximately 80% of the theoretical values and there is an optimal CNTs fraction to access the maximum mechanical properties. Chin et al [1] found that this amount is 0.15wt % for MWCNT/PC composites which is close to what we have obtained. According to Fig. 6, the variation of Young's modulus can be neglected in the range of 0.05-0.5 wt % of CNT concentration. It is reasonable to expect that at higher CNT loading (0.5-1.15 wt % in second percolation region) a strong mechanical reinforcement would be achieved where the CNTs contact directly by forming CNT network.

### 3.4 Electrical conductivity

The electrical conductivity of PC/MWCNT composites was measured and is plotted in (Fig. 7). One could divide the plot of conductivity with CNT weight fractions into four distinct regions. In region 1, the

conductivity increases with CNT content up to 0.1 wt% and afterwards it tends to flatten in the range of 0.1-0.7wt% (region 2). Then an increase of conductivity about 5 orders of magnitude occurs (region 3) while the CNT content passes from 0.7wt% to 1.15wt%. In region 4, the conductivity tends to saturate at the higher contents.

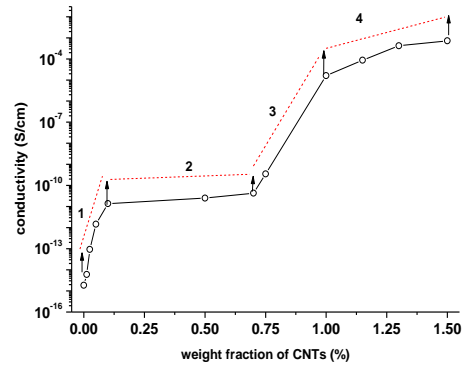


Fig. 7. Effect of MWCNT content on conductivity of PC/MWCNT composites.

At low CNT concentrations (region 1) in the composites, the electrical conductivity is due to the electron hopping phenomenon. An increase in the filler concentration (i.e. CNTs) results in considerably higher conductive sites that lead to easily electron hopping. The first percolation threshold (the critical concentration of CNTs based on percolation theory) [16] is estimated to be between 0.02 and 0.1 wt% in our case. When the concentration exceeds a certain value, the Van der Waals interaction between CNTs reduces the quality of uniform dispersion of individual CNTs by agglomeration and the rate of increment in conductivity (region 2). In fact, region 2 is a compromise between electron hopping effect and non-uniform dispersion of CNTs. (Fig. 8) clearly presents the agglomeration of various bundles of CNTs for 0.7 weight per cent.

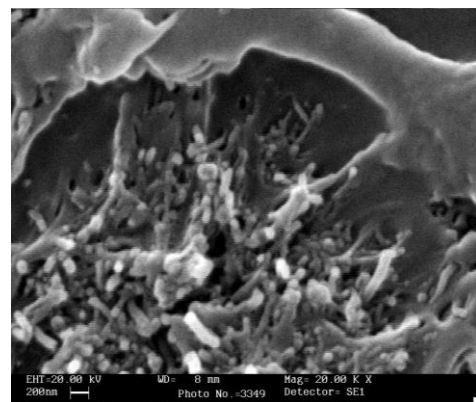


Fig. 8. SEM micrographs of PC/MWCNT composite of cryogenically cut film of 0.7 wt.%.

The sharp increase of conductivity in region 3 is probably due to contact between thin polymer coated or

uncoated CNTs which leads to an increase of path numbers between opposite sites and the formation of CNT networks. In this region, the second percolation threshold is expected to be between 0.7 and 1.0 wt%. Further increase of CNT content has a little effect on the number of CNT networks in the composite. Coleman et al [17] reported the percolation threshold of CNT/polymer composite for the first time. Rapid change in the conductivity related to filler load can be fully described by this theory, which it is concerning the dispersion of conductive fillers in the insulating matrix. According to our knowledge, no paper has reported two electrical percolation thresholds in thermoplastic based composites yet, while some publications [18, 19, 20] are reported such analogous behavior for epoxy based systems. In these publications, the formation of conductive networks is related to the mutual attraction of the nanotubes after addition of hardener, which is named kinematic percolation threshold. The shear induced force after hardener addition is the origin of the first threshold in their case [19].

Since Polycarbonate is a thermoplastic polymer which does not require a hardener, therefore the reason of the first threshold formation for it, can not be such as epoxy. As we have previously mentioned, it is related to the electron hopping effect in conductive sites. Also, they identified the second threshold as statistical percolation threshold which is independent of fabrication process [3]. In a composite consisting of conductive fillers in insulating matrix, the conductivity is estimated by the scaling law  $\sigma = A (w-w_c)^t$  where  $\sigma$  is conductivity of composite,  $w$  is weight fraction and  $w_c$  critical weight fraction of CNTs,  $A$  and  $t$  are constants which depend on conductivity of filler and the system dimensionality, respectively.

To obtain the constants of scaling model, the  $\log \sigma$  vs.  $\log (w-w_c)$  is plotted for two percolation thresholds in (Fig. 9) while varying  $w_c$  until the best linear fitting was obtained. As shown in this figure, the highly accurate fitting between power law equation and experimental results confirms percolation network of MWCNTs [21]. The first percolation constants (at 0.022) are  $A=8.03 \times 10^{-11}$  S/cm and  $t=1.09$  (Fig. 9a).

Taking into account of the reported values of  $t$  in the literature [3] for 2-D and 3-D systems which are 1.33 and 1.9 respectively, the low value of  $t$  calculated in our work does not indicate a reduction in system dimensionality but reflects the aggregation of CNTs during the sample preparation as shown in (Fig. 5a). A similar result is also reported by Sandler et al [18]. The second percolation constants (at 0.735wt %) are estimated to be  $A=2.51 \times 10^{-3}$  S/cm and  $t=3.7$  (Fig. 9b). It is demonstrated that there is electrically tunneling barrier between the filler particles due to coating of their surface with a thin layer of polymer in the solution phase [22]. An increase of this barrier may cause an excess of  $t$  value from 2, and a reduction of maximum conductivity ( $\sigma_{max}$ ) and  $A$  in comparison with filler conductivity [3].

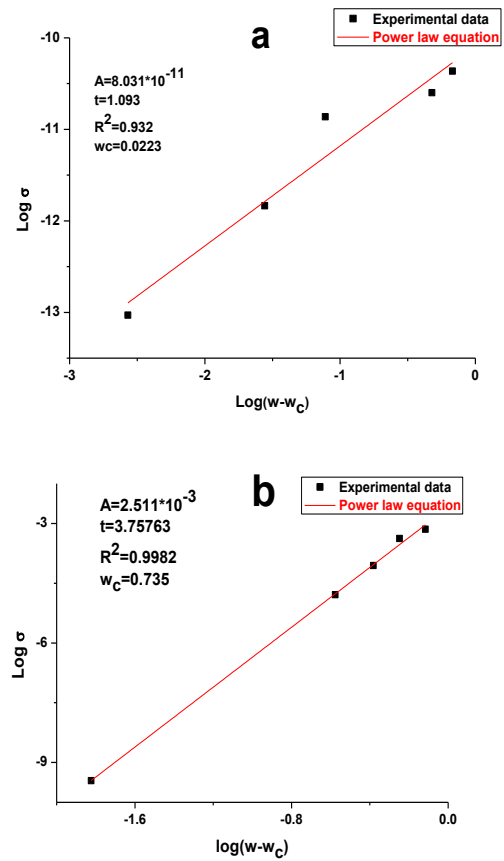


Fig. 9. The power fit in the percolation region, (a) after first threshold, (b) after second threshold.

Connor et al [23] suggested that if electrical conductivity would be dominated by quantum tunneling between CNTs, the following relation could be applied:

$$\ln(\sigma_{DC}) \approx -w^{-1/3} \quad (4)$$

Where  $\sigma_{DC}$  is conductivity obtained from DC measurements. (Fig. 10) shows the plot of the conductivity data obtained from (Fig. 7) vs.  $w^{-1/3}$ .

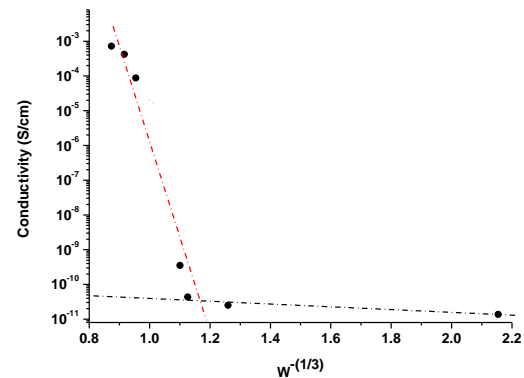


Fig. 10. Logarithmic plot of conductivity vs.  $w^{-1/3}$ .

As shown in this figure, the mentioned proportionality can be clearly specified in two separate domains,

corresponding to the first and second percolation thresholds. It is worth noting that at low CNT concentrations, the experimental results are well fitted with that of predicted by theory, however, it is not true in the case of above 0.7 wt% where a deviation from linearity is observed. This deviation is probably due to the fact that the mechanism of charge transport in this case is not only related to the tunneling through polymer barriers between CNTs, but to the direct contact between them as reported by Ounaies et al [24]. It is supposed that a greater direct contact between CNTs leads to larger deviation from linearity.

#### 4. Conclusions

The PC/MWCNT nanocomposites were prepared with solution casting technique. Effects of CNTs concentration on various properties of nanocomposites have been studied. It is found that increasing CNT concentration increased the electrical conduction of composites, while it reduced their transparency. However, satisfactory optical transparency was achieved in 0.1 wt% load of CNTs in composite. The modulus shows negligible improvement over the neat PC in the range of 0.05-0.5 wt %. The experimental data concerning the composite modulus nearly follow the theoretical values up to 0.13 wt%, but differ from this for higher filler concentration due to MWCNT aggregation which causes a reduction in dispersion uniformity. From the conductivity results, two percolation thresholds in PC/MWCNT composites analogous to epoxy based systems were revealed. Also, the experimental conductivity followed a scaling law in the percolation regions. A conductivity plateau was observed in our case which was attributed to a compromise between electron hopping and non-uniform dispersion of CNTs.

#### References

- [1] Y. C. Chin, MSC Thesis, the Florida state university, Department of Mechanical Engineering (2007).
- [2] S. M. Yuen, C. C. M. Ma, C. Y. Chuang, Y. H. Hsiao, C. L. Chiang, A. D. Yu, *Composites: Part A*. **39**, 119 (2008).
- [3] Q. Wang, J. Dai, W. Li, Z. Wei, J. Jiang, *Composite Science and Technology*. **68**, 1644 (2008).
- [4] W. Bauhofer, J. Z. Kovacs, *Composite Science and Technology*. **69**, 1486 (2009).
- [5] B. Lin, U. Sundararaj, P. Po'tschke, *Macromolecular Materials and Engineering*. **69**, 227 (2006).
- [6] S. Wang, Z. Liang, G. Pham, Y. B. Park, B. Wang, C. Zhang, L. Kramer, P. Funchessn, *Nanotechnology*, **18**, 5708 (2007).
- [7] D. H. Park, K. H. Yoon, Y. B. Park, Y. S. Lee, Y. J. Lee, S. W. Kim, *Journal of Applied polymer Science*. **113**, 450 (2009).
- [8] P. Delhaes, M. Couzi, M. Trinquescoste, J. Dentzer, H. Hamidou, C. V. Guterl, *Carbon*. **44**, 3005 (2006).
- [9] J. C. Halpin, J. Kardos, *Polymer Engineering Science*. **16**, 344 (1976).
- [10] G. Overney, W. Zhong, D. Tomanek, *Zeitschrift Fur Physik D-Atoms Molecules and Clusters*. **27**, 93 (1993).
- [11] J. Bernholc, C. Brabec, M. B. Nardelli, A. Maiti, C. Roland, B. I. Yakobson, *Applied Physics A-Materials*. **67**, 39 (1998).
- [12] E. T. Thostenson, Z. Ren, T. W. Chou. *Composite Science and Technology*. **61**, 1899 (2001).
- [13] N. Hu, Z. Masuda, G. Yamamoto, H. Fukunaga, T. Hashida, J. Qiu, *Composite Part A-Applide Science*. **39**, 893 (2008).
- [14] R. F. Gibson, *Principals of composite material mechanic*, Mc. Graw Hill (1994).
- [15] S. Singh, Y. Pei, R. Miller, P. R. Sundarajan. *Advanced Functionalized Materials*. **13**, 868 (2003).
- [16] D. Stauffer, A. Aharony, *Introduction to Percolation theory*, Taylor & Francis, London (2003).
- [17] J. N. Coleman, S. Curran, A. B. Dalton, A. P. Davey, B. McCarthy, W. Blau, R. C. Barklie, *Physical Review B*. **58**, 7492 (1998).
- [18] J. K. W. Sandler, J. E. Kirk, I. A. Kinloch, M. S. P. Shaffer, A. H. Windle, *Polymer*. **44**, 5893 (2003).
- [19] J. Z. Kovacs, B. S. Velagala, K. Schulte, W. Bauhofer, *Composite Science and Technology*. **67**, 922 (2007).
- [20] M. B. Bryning, M. F. Islam, J. M. Kikkawa, A. G. Yodh, *Advanced Materials*. **17**, 1186 (2005).
- [21] I. O'Connor, S. De, J. N. Coleman, Y. K. Gun'ko, *Carbon*. **47**, 1983 (2009).
- [22] Y. R. Hernandez, A. Grynson, F. Blighe, M. Cadec, V. Nicolosi, W. Blau, Y. Gun'ko, J. Coleman, *Scripta Material*. **58**, 69 (2008).
- [23] M. T. Connor, S. Roy, T. A. Ezquerra, F. B. Calleja, *Physical Review B*. **57**, 2286 (1998).
- [24] Z. Ounaies, C. Park, K. E. Wise, E. J. Siochi, J. S. Harrison, *Composite Science and Technology*. **63**, 1637 (2003).

\*Corresponding author: mmojtahedzadeh@nrcam.org